ACS Macro Letters

Letter

pubs.acs.org/macroletters

Photocleavable Triblock Copolymers Featuring an Activated Ester Middle Block: "One-Step" Synthesis and Application as Locally Reactive Nanoporous Thin Films

Hui Zhao,[†] Weiyin Gu,[‡] Ryohei Kakuchi,[†] Zhiwei Sun,[‡] Elizabeth Sterner,[‡] Thomas P. Russell,[‡] E. Bryan Coughlin,*[,‡] and Patrick Theato*[,†]

[†]Institute for Technical and Macromolecular Chemistry, University of Hamburg, Bundesstr.45, 20146 Hamburg, Germany

[‡]Department of Polymer Science and Engineering, University of Massachusetts, 120 Governors Drive, Amherst, Massachusetts 01003-4530, United States

Supporting Information

ABSTRACT: Polystyrene-*block*-poly(maleimide pentafluorophenyl ester-*co*-styrene)-*block*-poly(ethylene oxide) with an *o*-nitrobenzyl ester junction was synthesized by "one-step" RAFT polymerization. Highly ordered and locally reactive nanoporous thin films were obtained from the photocleavable triblock copolymer after spin coating, solvent annealing, UV exposure, and washing with methanol/water to remove the minor block PEO. The local reactivity in the thin films was demonstrated by fabrication of iron oxide nanotori after post-modification with an amino-functionalized ferrocene and treatment with oxygen plasma.

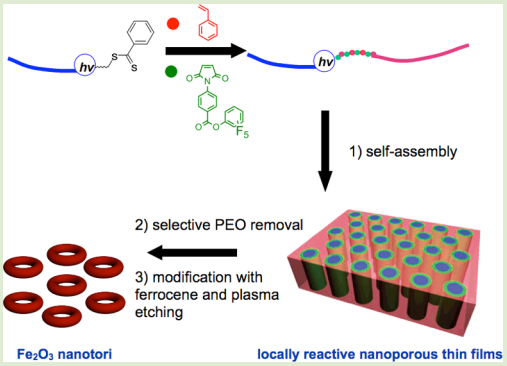

Nanoporous thin films have attracted sustained interest for their potential applications as templates,[1] separation materials,[2] and other advanced applications.[3] Decorating the pore walls with reactive functional groups is critically important for nanoporous film applications for specific post-modification and host−guest interactions.[4] Several strategies have been developed for fabrication of porous thins featuring reactive pores. For example, Russell and co-workers reported nanoporous thin films from polystyrene-*block*-poly(ethylene oxide) with a disulfide group as a junction.[5] The porous structures with thiol groups on the surface of pores were formed after D,L-dithiothreitol treatment and methanol washing. This kind of diblock copolymer with a protected reactive junction group provided a facial method to fabricate reactive nanoporous thin films. However, the density of pore surface functional groups introduced by this strategy is relatively low, which hinders further advanced applications of the reactive thin films.

Higher densities of pore surface functionality can be obtained from triblock copolymer with a reactive middle block. However, the synthesis of these copolymers often involve multistep reactions, which is challenging. For example, Hillmyer and co-workers synthesized polystyrene-*block*-poly(dimethylacrylamide)-*block*-polylactide, in which the midblock poly(dimethylacrylamide) was transformed to poly(acylic acid) after hydrolysis.[6] Additionally, the reported functional groups on the pore walls in the thin films were only partially active and only reacted under limited conditions. Hence, there is a strong demand for efficient, yet simple, synthetic routes toward nanoporous thin films that exhibit high-density reactive functional groups on the pore walls.

In this work, as outlined in Figure 1A, a "one-step" synthetic route was developed to synthesize photocleavable triblock copolymers featuring a reactive middle block with pentafluorophenyl ester groups. Our approach is based on the well-known alternating copolymerization of styrene and maleimide.[7] By using an excess of styrene monomer, copolymerization with a functionalized maleimide while using a poly(ethyl oxide) (PEO) based chain transfer agent is expected to produce a triblock copolymer with reactive ester middle block in one step. The present triblock copolymer has three advantages: (a) "one-pot−one-step" synthesis, avoiding multisteps polymerization and purification; (b) incorporating a photocleavable junction on the basis of an *o*-nitrobenzyl ester, between PEO and poly(styrene-*co*-maleimide)-*block*-polystyrene, allowing the fabrication of highly ordered nanoporous thin films under mild conditions,[8] (c) positioning of reactive pentafluorophenyl ester groups, which are known to react quantitatively with amines, providing an efficient route to post-modification of the materials. Therefore, it is very promising candidate to produce locally reactive nanoporous thin films from the proposed triblock copolymer (Figure 1C).[9]

Received: July 25, 2013
Accepted: October 11, 2013
Published: October 14, 2013

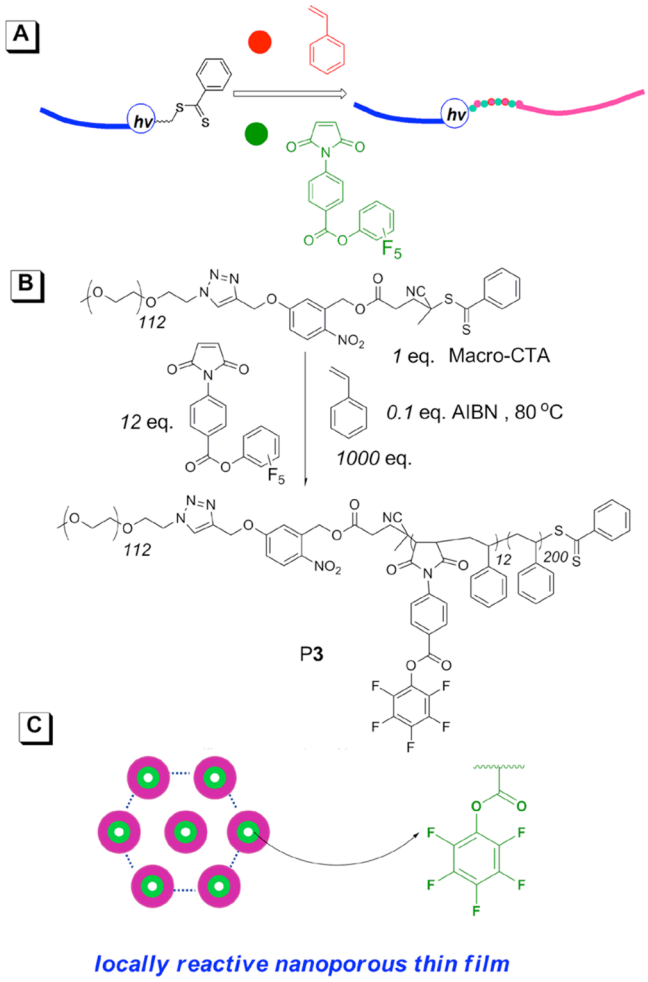

Figure 1. (A) Concept for "one-step" RAFT polymerization to triblock copolymer. (B) Synthetic scheme for photocleavable triblock copolymer with activated esters junction block. (C) Locally reactive patterns from P3.

A poly(ethyl oxide) (PEO) chain transfer agent with an *o*-nitrobenzyl ester (ONB) junction (Macro-CTA) was synthesized by CuAAC click reaction.[8d] Next, the RAFT polymerization of styrene in the presence of pentafluorophenyl 4-maleimidobenzoate (MAIPFP) and Macro-CTA was performed in bulk at 80 °C under an argon atmosphere with a ratio of $[St]_0/[\ MAIPFP\ ]_0/[Macro\text{-}CTA]_0$ being 1000:12:1 (run 3 in Table 1). The polymerization kinetics were investigated by means of ^{1}H NMR measurements. MAIPFP conversion reached 100% within 25 min, while the conversion of styrene was only 6% after that time. Notably, the polymerization rate of styrene is slow (the conversion reached around 20% after 16 h), but the polymerization was still proceeding after all MAIPFP monomer was consumed in a controlled manner. (Figure 2A). The polymerization kinetics clearly demonstrates that the MAIPFP monomer was consumed in the early stage during the copolymerization with styrene, indicating that the MAIPFP monomer was precisely incorporated in an alternating fashion resulting in the middle block between PEO block and PS block. The length of the middle block can also be controlled by changing the ratio between MAIPFP and CTA. For example, as shown in Figure 2B, the ^{1}H NMR proton ratio between maleimide aromatic proton resonance and the end-group of PEO *d* was 10:1, which corresponds to 15 MAIPFP units in the polymer. This value of MAIPFP units is in good agreement with the feed ratio between MAIPFP and Macro-CTA, which in this case was 12:1. Other data on varying the middle block length are summarized in Table 1.

Table 1. RAFT Polymerization of Styrene and MAIPFP[a]

polymer	MAIPFP $Unit_{NMR}$[b]	MAIPFP $unit_{theory}$	M_n[c] g/mol	M_w[c] g/mol	$Đ$[c]
P1	4.5	3	30300	35800	1.17
P2	11.5	9	27300	32000	1.16
P3	15.1	12	28100	33800	1.18
P4	34.4	24	30200	35000	1.20

[a]Bulk, 80 °C, 15 h, styrene conversion = 18−20%, MAIPFP conversion = 100% (at 25 min, MAIPFP conversion = 100%) determined by ^{1}H NMR in $CDCl_3$. [b]Determined by ^{1}H NMR in $CDCl_3$. [c]GPC in THF using linear PS standards.

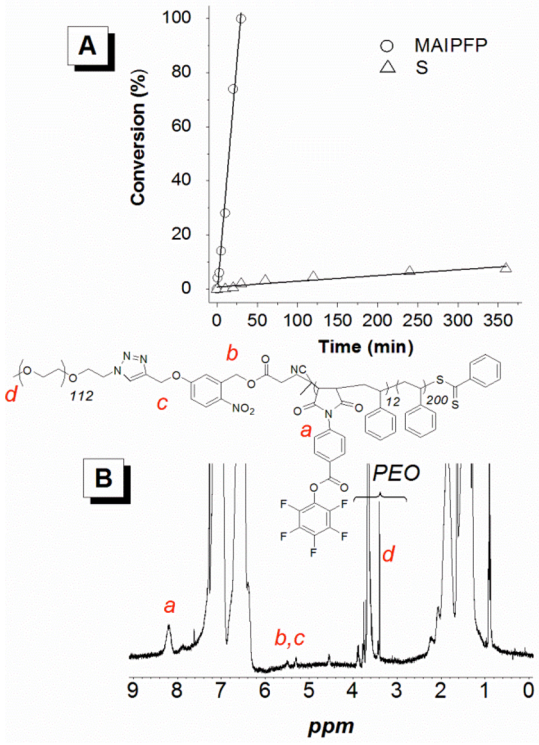

Figure 2. (A) Kinetic plots for polymerization of styrene in the presence of MAIPFP, determined by ^{1}H NMR. (B) ^{1}H NMR of triblock copolymer PEO-*b*-P(S-*co*-MAIPFP)-*b*-PS (P1) in $CDCl_3$.

Next, photocleavage was investigated by GPC. P3 (10 mg/mL) was exposed in a NMR tube to a UV source (6W, 365 nm) for 12 h. In Figure S1, GPC analysis shows the successful photocleavage of P3. After UV irradiation, the GPC elution peak associated with block copolymers (33800 g/mol) split into lower molecular weight peaks (20100 and 7000 g/mol), which were assigned to the cleaved P(MAIPFP-*co*-S)-*b*-PS and PEO.

Motivated by these results, thin films of the triblock copolymer P3 were investigated. Among the four polymers, we have chosen the polymer P3 with the highest MAIPFP content that is still capable of forming highly ordered hexagonally packed cylinders (P4 with higher MAIPFP than P3 did not form long-range highly ordered packing, see

dx.doi.org/10.1021/mz400389r | *ACS Macro Lett.* 2013, 2, 966−969

Supporting Information S5). A 35 nm thick BCP thin film was prepared by spin-coating a solution of 0.8 wt % of P3 in toluene onto silicon substrates. Subsequently, the film was annealed in a THF/water vapor environment. The surface morphology of the annealed thin film was determined by atomic force microscopy (AFM) as shown in Figure 3. Highly ordered hexagonally

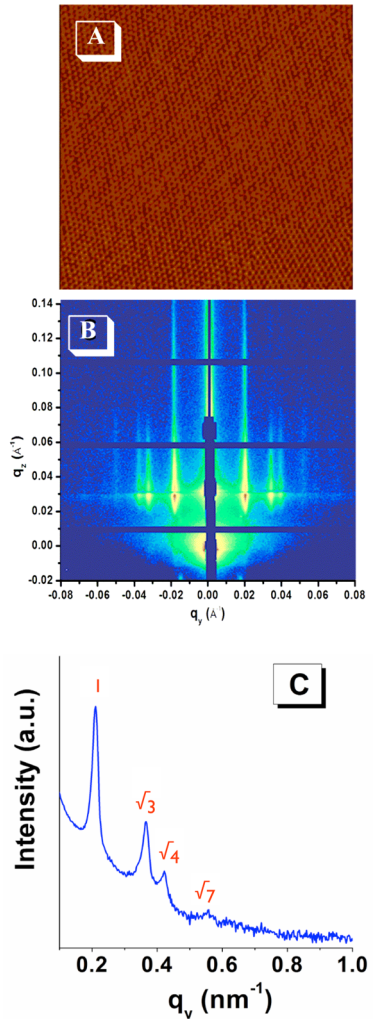

Figure 3. (A) AFM image for P3 thin film after water/THF annealing 2.5 h. (B) GISAXS patterns for P3 thin film. (C) Intensity scan along q_y of the GISAXS patterns shown in (B).

packed arrays indicate that PEO cylinders were oriented normal to the substrate, similar to thin films of PS-*b*-PEO copolymers. Static grazing incidence small-angle X-ray scattering (GISAXS) was used to characterize the thin films over large area. An incidence angle of 0.2°, which is between the critical angle of polymer (0.16°) and silicon substrate (0.28°), was chosen so that the X-ray can penetrate into the film, where the scattering profiles are characteristic of the entire film. The corresponding 2D GISAXS pattern is shown in Figure 3B. In the data, q_y represents the momentum transferred normal to the incident plane, that is, parallel to the thin film surface, while q_z is normal to the sample surface. Brag rods (reflections extended along q_z) are observed, which are characteristic of cylindrical microdomains oriented normal to the film surface. The observed multiple order reflection peaks are characteristic of long-range ordering. A line scan in q_y is shown in Figure 3C. The first order reflection was at $q^* = 0.205$ nm^{-1} and the d spacing is calculated to be 31 nm. Highly ordered nanoporous thin films were obtained after UV exposure and a successive washing with MeOH to selectively remove the PEO block. As can be seen from TEM images in Figure S2A, the nanoporous morphology can be directly observed without the need for any staining due to the large difference in electron density between the matrix and the empty pores. An average pore diameter of 16 nm and an average center-to-center distance between the pores of 35 nm were obtained. These values are in good agreement with the GISAXS data.

To demonstrate the presence of reactive functional groups on the pore walls, the nanoporous film was immersed into an ethanol solution of 2-aminoethyl-ferrocene (Fc-amine), anchoring Fc-amine to the pore walls via the activated esters-amine conjugation chemistries (for details, see experimental section in Supporting Information). The modified nanoporous films were then treated with oxygen plasma to decompose all the organic materials, while converting ferrocence to iron oxide at the same time (Figures S2B and S2C). Hence, this approach is to establish an access to the pore wall functionalities and should provide a higher number of functional groups compared to previous methods. While analysis of reactive groups within a block copolymer film is tedious, we propose this indirect proof by converting the block copolymer film structure into Fe_2O_3 nanostructures, replicating the location of iron sources within the block copolymer film. Accordingly, nanotori (also called nanorings or nanodonuts) are expected. However, against our expectation, as shown in Figures S2B and S2C, we observed highly ordered nanodots with a diameter of around 20 nm. To explore the origin of nanodots formation rather than nanotori, TEM images were taken after Fc-amine modification and washing with methanol. As shown in Figure S3A, the Fc-amine appeared to be aggregated in the center of the open pores rather than decorating the pore walls. This could be the result of unfavorable interactions between the hydrophilic Fc-amine and the hydrophobic pore walls. Further, residual PEG in the pores could also absorb Fc-amine via hydrogen bonding, which could be another reason for the formation of nanodots. The physically aggregated Fc-amine can be removed after immersing the thin film into 0.1 M HCl solution for 3 h (Figure S3B). However, we did not see nanotori in the TEM post-acid washing. The electron density contrast between the Fc-amine functionalized pore walls and the PS matrix may not be sufficient to observe these sub-10 nm features. Finally, this post-acid washing sample was treated with oxygen plasma, during which the functionalized porous thin film was transformed to iron oxide nanotori. The structures were characterized by AFM and the result is shown in Figure 4. Clearly nanotori were observed and the average diameter of the tori was around 39 nm with average height around 1 nm. The tori had around 7 nm wall thicknesses. The height of the nanodots was around 8 nm, while the height of the nanotori was around 1 nm. Both heights are much smaller than their parent film thickness. This is because the thin film structures will likely collapse after the plasma-O_2 etching step. Besides, the density of the Fc-amines on the pore walls after the post-modification is much lower than those trapped in the pores leading to nanodots. This can be seen from TEM results (Figure S3). Consequently, the smaller height of nanotori compared to the nanodots can be understood. In summary, these structures result from the activated esters located at the wall of the copolymer films pores. The structure of the obtained tori supports our assertion that the alternating styrene-

dx.doi.org/10.1021/mz400389r | *ACS Macro Lett.* 2013, 2, 966−969

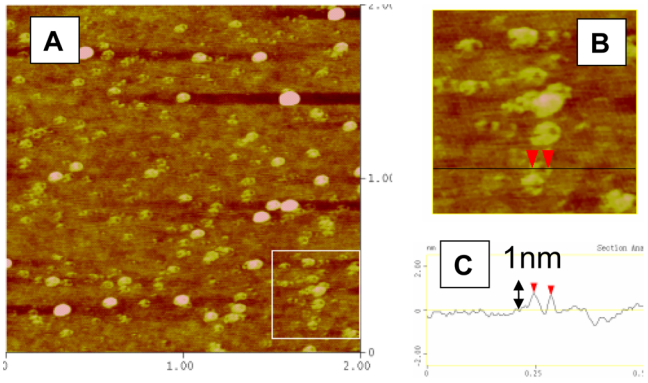

Figure 4. (A, B) AFM height images for iron oxide nanotori. Scales: A, 2 × 2 μm^2; B, 0.5 × 0.5 μm^2. (C) Height profile in B, height scale is 1 nm.

maleimide served a reactive middle block between PEO and PS. A control experiment under the same conditions with a photocleavable diblock copolymer PS-*hv*-PEO, which essentially lacks the reactive middle block, did not result in nanotori (see Supporting Information).

The resulting nanotori were characterized by high resolution X-ray photoelectron spectroscopy (XPS). The results are shown in Figure S4. Two binding peaks can be seen at 725 and 710 eV, which were assigned to Fe 2p and Fe $2p_{1/2}$ in a γ-Fe_2O_3 sample, respectively. The XPS measurement once again demonstrates that we successfully post-modified the thin films with Fc-amine.

In conclusion, we have demonstrated the synthesis of a functional and photocleavable triblock copolymer with an activated ester middle block was prepared in a one-step reaction. Further, activated ester-functionalized nanopores were generated by photocleavage and solvent extraction. The active ester functionalities at the interface between the matrix and pore walls could then be used as reactive handles to generate iron oxide nanotori. The results in this work present a unique example of a mild etching process and interface functionalization based on *o*-nirtrobenzyl ester and activated ester chemistries. As such, the method described here provides a broad range of possibilities, because the reactive middle block can easily be functionalized with a large variety of amines that can lead to interesting applications in patterned materials.

■ ASSOCIATED CONTENT

Supporting Information

Experimental section, characterization data (NMR, AFM, XPS), general procedures for RAFT polymerization, preparation of the thin films, and fabrication iron nanotori from thin films. This material is available free of charge via the Internet at http://pubs.acs.org.

■ AUTHOR INFORMATION

Corresponding Author

*E-mail: theato@chemie.uni-hamburg.de; coughin@mail.pse.umass.edu.

Notes

The authors declare no competing financial interest.

■ ACKNOWLEDGMENTS

Financial support from the German Science Foundation (DFG) under Grant TH 1104/4-1 and an International Collaboration in Chemistry award from the National Science Foundation (CHE 0924435) is gratefully acknowledged. This research was partly supported by the WCU (World Class University) program through the National Research Foundation of Korea funded by the Ministry of Education, Science and Technology (R31-10013). The self-assembly and ordering of the BCPs was performed by W.G. and T.P.R. who are supported by the U.S. Department of Energy (DOE) under DOE DE-FG02-96ER45612.

■ REFERENCES

(1) (a) Tseng, W. H.; Chen, C. K.; Chiang, Y. W.; Ho, R. M.; Akasaka, S.; Hasegawa, H. *J. Am. Chem. Soc.* **2009**, *131*, 1356. (b) Jones, B. H.; Lodge, T. P. *Chem. Mater.* **2010**, *22*, 1279. (c) Crossland, E. J. W.; Kamperman, M.; Nedelcu, M.; Ducati, C.; Wiesner, U.; Smilgies, D. M.; Toombes, G. E. S.; Hillmyer, M. A.; Ludwigs, S.; Steiner, U.; Snaith, H. J. *Nano Lett.* **2009**, *9*, 2807. (d) Melde, B. J.; Burkett, S. L.; Xu, T.; Goldbach, J. T.; Russell, T. P.; Hawker, C. J. *Chem. Mater.* **2005**, *17*, 4743. (e) Crossland, E. J. W.; Ludwigs, S.; Hillmyer, M. A.; Steiner, U. *Soft Matter* **2007**, *3*, 94.

(2) (a) Jackson, E. A.; Hillmyer, M. A. *ACS Nano* **2010**, *4*, 3548. (b) Wang, X.; Husson, S. M.; Qian, X.; Wickramasinghe, S. R. *J. Membr. Sci.* **2010**, *365*, 302. (c) Phillip, W.; Rzayev, J.; Hillmyer, M.; Cussler, E. *J. Membr. Sci.* **2006**, *286*, 144. (d) Phillip, W. A.; O'Neill, B.; Rodwogin, M.; Hillmyer, M. A.; Cussler, E. L. *ACS Appl. Mater. Interfaces* **2010**, *2*, 847.

(3) (a) Pulko, I.; Wall, J.; Krajnc, P.; Cameron, N. R. *Chem.—Eur. J.* **2010**, *16*, 2350. (b) Kimmins, S. D.; Cameron, N. R. *Adv. Funct. Mater.* **2011**, *21*, 211. (c) Zhang, Y.; Wang, S.; Eghtedari, M.; Motamedi, M.; Kotov, N. A. *Adv. Funct. Mater.* **2005**, *15*, 725. (c) Hu, X.; Li, G.; Li, M.; Huang, J.; Li, Y.; Gao, Y.; Zhang, Y. *Adv. Funct. Mater.* **2008**, *18*, 575.

(4) Wu, D.; Xu, F.; Sun, B.; Fu, R.; He, H.; Matyjaszewski, K. *Chem. Rev.* **2012**, *112*, 3959.

(5) Ryu, J. H.; Park, S.; Kim, B.; Klaikherd, A.; Russell, T. P.; Thayumanavan, S. *J. Am. Chem. Soc.* **2009**, *131*, 9870.

(6) Rzayev, J.; Hillmyer, M. A. *J. Am. Chem. Soc.* **2005**, *127*, 13373.

(7) (a) Alfrey, T.; Lavin, E. *J. Am. Chem. Soc.* **1945**, *67*, 2044. (b) Pfeifer, S.; Lutz, J.-F. *J. Am. Chem. Soc.* **2007**, *129*, 9542. (c) Weiss, J.; Li, A.; Wischerhoff, E.; Laschewsky, A. *Polym. Chem.* **2012**, *3*, 352.

(8) Nanoporous thin films from photocleavable BCPs based on ONB junctions, see: (a) Kang, M.; Moon, B. *Macromolecules* **2009**, *42*, 455. (b) Schumers, J. M.; Vald, A.; Huynen, S.; Gohy, J. F.; Fustin, C. A. *Macromol. Rapid Commun.* **2011**, *3*, 199. (c) Zhao, H.; Gu, W.; Sterner, E.; Russell, T. P.; Coughlin, E. B.; Theato, P. *Macromolecules* **2011**, *44*, 6433. (d) Zhao, H.; Gu, W.; Thielke, M. W.; Sterner, E.; Tsai, T.; Russell, T. P.; Coughlin, E. B.; Theato, P. *Macromolecules* **2013**, *46*, 5195. (e) Zhao, H.; Sterner, E.; Coughlin, E. B.; Theato, P. *Macromolecules* **2012**, *45*, 1723. (f) Gu, W.; Zhao, H.; Wei, Q.; Coughlin, E. B; Theato, P.; Russell, T. P. *Adv. Mater.* **2013**, *25*, 4690.

(9) (a) Theato, P. *J. Polym. Sci., Part A: Polym. Chem.* **2008**, *46*, 6677. (b) Theato, P., Klok, H. A., Eds. *Funtional Polymer by Post-polymerization on Modification: Concepts, Guideline and Application*; Wiley-VCH, Weinheim, 2012. (c) Guenay, K. A.; Theato, P.; Klok, H. A. *J. Polym. Sci., Part A: Polym. Chem.* **2013**, *51*, 1.